Journal of Systems Engineering and Electronics
Vol. 32, No. 6, December 2021, pp.1354 – 1363

Underdetermined DOA estimation via multiple time-delay covariance matrices and deep residual network

CHEN Ying, WANG Xiang*, and HUANG Zhitao

State Key Laboratory of Complex Electromagnetic Environment Effects on Electronics and Information System, National University of Defense Technology, Changsha 410073, China

Abstract: Higher-order statistics based approaches and signal sparseness based approaches have emerged in recent decades to resolve the underdetermined direction-of-arrival (DOA) estimation problem. These model-based methods face great challenges in practical applications due to high computational complexity and dependence on ideal assumptions. This paper presents an effective DOA estimation approach based on a deep residual network (DRN) for the underdetermined case. We first extract an input feature from a new matrix calculated by stacking several covariance matrices corresponding to different time delays. We then provide the input feature to the trained DRN to construct the super resolution spectrum. The DRN learns the mapping relationship between the input feature and the spatial spectrum by training. The proposed approach is superior to existing model-based estimation methods in terms of calculation efficiency, independence of source sparseness and adaptive capacity to non-ideal conditions (e.g., low signal to noise ratio, short bit sequence). Simulations demonstrate the validity and strong performance of the proposed algorithm on both overdetermined and underdetermined cases.

Keywords: direction-of-arrival (DOA) estimation, underdetermined condition, deep residual network (DRN), time delay, covariance matrix.

DOI: 10.23919/JSEE.2021.000115

1. Introduction

In various fields, such as wireless communication, radar, astronomical observation, and exploration, direction-of-arrival (DOA) estimation is always a significant research hotspot. Existing methods include beamforming algorithms [1], maximum likelihood algorithms [2], subspace algorithms [3,4], and sparse reconstruction algorithms [5,6], which have been utilized for DOA estimation, but they do not perform well under so-called underdetermined conditions (i.e., where there are fewer sensors than sources), which renders them inapplicable in some cases such as multiple targets communication surveillance.

The multiple signal classification (MUSIC)-like algorithm based on fourth-order cumulant (FO-MUSIC) [7] has been developed for meeting the demand of undetermined DOA estimation. Physical arrays can generate many virtual sensors via this algorithm, thereby achieving higher degrees of freedom. This algorithm has also been extended to an arbitrary even order $2q(q>1)$ to further enhance its resolution and increase the number of sources that can be estimated [8]. Other effective approaches [9−14] have also been proposed to deal with the DOA estimation problem on underdetermined cases. However, these model-based methods rely on many qualifications, such as a sufficiently long bit sequence length (BSL), high signal to noise ratio (SNR) or ideal distribution properties of signals. In the actual DOA estimation process, these pre-suppositional conditions are rather restrictive and difficult to be satisfied. Meanwhile, these model-based methods are very computationally complex as well due to the higher-order cumulant calculation procedures and multiple iterations.

The deep-learning (DL) based approach is considered one of the most effective technical solutions to DOA estimation. These methods have advantages in computational complexity, estimation accuracy, and adaptability to non-ideal cases [15−25]. In [18], a framework of a multitask auto-encoder and a series of parallel multilayer classifiers were developed for super-resolution DOA estimation. This method has been proven adaptable to a variety of array errors. Xiang et al. [21] proposed a phase enhancement approach based on deep neural network (DNN) to deal with DOA estimation problems in multipath environments. In [23], an efficient deep convolution network (DCN)-based method was established to

Manuscript received February 19, 2021.
*Corresponding author.
This work was supported by the Program for Innovative Research Groups of the Hunan Provincial Natural Science Foundation of China (2019JJ10004).

learn the sparse linear inverse transformation from array outputs to DOA spectra. Simulation results have shown that DL-based methods consistently outperform model-driven methods.

Motivated by the advantages of DL-based methods, this paper presents a deep residual network (DRN)-based method to solve DOA estimation problems in underdetermined cases. An expanded second-order (SO) statistic deduced by multiple time-delay covariance matrices of the array output serves as the input of the DRN. This input feature extraction procedure adopts the idea of stacking multiple covariance matrices corresponding to different time delays [26−28]. The DRN can learn the nonlinear mapping relationship between the input feature and the spatial spectrum by training without necessitating an accurate direction estimation model [29]. When the offline training process is complete, online testing can be efficiently implemented by hardware in parallel. Thus, the proposed method has significant advantages in terms of computational efficiency. Moreover, the proposed method is independent on the precise mathematical model because of the end-to-end learning process, thus showing a better robustness in practical applications.

The remainder of this paper is organized as follows. In Section 2, we formulate the underdetermined DOA estimation problem. In Section 3, the proposed DRN-based DOA estimation algorithm is described. In Section 4, the excellent performance of the DRN-based method is shown through contrast experiments. Section 5 draws conclusions.

2. Problem formulation

We presume that J independent far-field signals $\boldsymbol{s}(t)=[s_1(t),s_2(t),\cdots,s_J(t)]^{\mathrm{T}}$ are incident on an N sensor uniform linear array (ULA) simultaneously. There is no mutual coupling or channel inconsistency interference between the array sensors. Then, the array output at t can be expressed as

$$\boldsymbol{x}(t)=\sum_{j=1}^{J}\boldsymbol{a}_j s_j(t)+\boldsymbol{v}(t)=\boldsymbol{A}\boldsymbol{s}(t)+\boldsymbol{v}(t) \tag{1}$$

where $t=t_1,t_2\cdots,t_B$, B is the number of snapshots, $\boldsymbol{A}=[\boldsymbol{a}_1,\boldsymbol{a}_2,\cdots,\boldsymbol{a}_J]$ is the array manifold matrix, $\boldsymbol{a}_j=\left[1,\mathrm{e}^{-\mathrm{j}2\pi\frac{1}{\lambda}d\sin\theta_j},\cdots,\mathrm{e}^{-\mathrm{j}2\pi\frac{1}{\lambda}(N-1)d\sin\theta_j}\right]^{\mathrm{T}}$ is the response vector corresponding to θ_j, d is the size of the sensor interval, λ is the length of waves, $\boldsymbol{v}(t)$ represents the zero-mean Gaussian white noise and $(\cdot)^{\mathrm{T}}$ is the transpose operator.

In an underdetermined case, $J>N$. The problem to be solved is the estimation of the angle set $\boldsymbol{\theta}=[\theta_1,\theta_2,\cdots,\theta_J]$ from the array output in the case $J>N$. Many effective methods have been proposed to solve such problems, but they tend to have excessive computational complexity and stability problems under short bit sequences and low-SNR conditions. Thus, we seek to achieve super-resolution DOA estimation via array outputs with DL technology.

3. Proposed algorithm

In this section, we propose an original DOA estimation method based on multiple time-delay covariance matrices and the DRN. The proposed method can be broken up into two main steps: (i) input feature extraction; (ii) deep network based DOA estimation.

3.1 Input feature extraction based on multiple time-delay covariance matrices

The covariance matrix corresponding to time delay τ_m is

$$\begin{aligned}\boldsymbol{C}_m&=\mathrm{E}\left\{\boldsymbol{x}(t)\boldsymbol{x}^{\mathrm{H}}(t+\tau_m)\right\}=\boldsymbol{A}\mathrm{E}\left\{\boldsymbol{s}(t)\boldsymbol{s}^{\mathrm{H}}(t+\tau_m)\right\}\boldsymbol{A}^{\mathrm{H}}=\\&\boldsymbol{A}\mathrm{diag}\left\{r_{s_1s_1^*}(\tau_m),r_{s_2s_2^*}(\tau_m),\cdots,r_{s_Ks_K^*}(\tau_m)\right\}\boldsymbol{A}^{\mathrm{H}}=\boldsymbol{A}\boldsymbol{D}_m\boldsymbol{A}^{\mathrm{H}}\end{aligned} \tag{2}$$

where $m=1,2,\cdots,M$, $(\cdot)^{\mathrm{H}}$ represents the Hermitian transpose operator. The noise term rejected for simplicity is regarded as a perturbation of (2). The matrices $\boldsymbol{C}_1,\boldsymbol{C}_2,\cdots,\boldsymbol{C}_M$ can be stacked in a matrix $\boldsymbol{C}\in\mathbb{C}^{N^2\times M}$ as follows:

$$\begin{aligned}&(\boldsymbol{C})_{(i-1)\times N+j,m}=(\boldsymbol{C}_m)_{ij},\\&i=1,2,\cdots,N;\ j=1,2,\cdots,N;\ m=1,2,\cdots,M.\end{aligned} \tag{3}$$

Define a matrix $\boldsymbol{D}\in\mathbb{C}^{M\times J}$ by $(\boldsymbol{D})_{mj}=(\boldsymbol{D}_m)_{jj}$, $m=1,2,\cdots,M$, $j=1,2,\cdots,J$, then $\boldsymbol{C}$ can be constructed as

$$\begin{aligned}\boldsymbol{C}&=[\boldsymbol{a}_1(\theta_1)\otimes\boldsymbol{a}_1^*(\theta_1),\cdots,\boldsymbol{a}_J(\theta_J)\otimes\boldsymbol{a}_J^*(\theta_J)]\boldsymbol{D}^{\mathrm{T}}=\\&(\boldsymbol{A}\odot\boldsymbol{A}^*)\boldsymbol{D}^{\mathrm{T}}\end{aligned} \tag{4}$$

where $\otimes$ represents the Kronecker product and $\odot$ represents the Khatri-Rao product.

After above analysis, the problem is transformed into the estimation of $\boldsymbol{\theta}$ from $\boldsymbol{C}$. To solve this problem, we first compute the correlation matrix $\boldsymbol{R}_{\boldsymbol{C}}$ as

$$\boldsymbol{R}_{\boldsymbol{C}}=\boldsymbol{C}\boldsymbol{C}^{\mathrm{H}}=(\boldsymbol{A}\odot\boldsymbol{A}^*)\boldsymbol{R}_{\boldsymbol{D}}(\boldsymbol{A}\odot\boldsymbol{A}^*)^{\mathrm{H}} \tag{5}$$

where $\boldsymbol{R}_{\boldsymbol{D}}=\boldsymbol{D}^{\mathrm{T}}\boldsymbol{D}^*$.

$\boldsymbol{R}_{\boldsymbol{C}}$ is a conjugate symmetric matrix and its diagonal elements contain unknown noise information, so select the off-diagonal upper right elements of $\boldsymbol{R}_{\boldsymbol{C}}$ to extract input feature $\tilde{\boldsymbol{R}}_{\boldsymbol{C}}$:

$$\begin{aligned}\tilde{\boldsymbol{R}}_{\boldsymbol{C}}=&[R_{1,2},R_{1,3},\cdots,R_{1,N},R_{2,3},\cdots,\\&R_{2,N},\cdots,R_{N-1,N}]^{\mathrm{T}}\in\mathbb{C}^{(N^2-1)N^2/2\times1}\end{aligned} \tag{6}$$

$$\bar{\boldsymbol{R}}=\begin{bmatrix}\text{real}(\tilde{\boldsymbol{R}}_C/\text{norm}(\tilde{\boldsymbol{R}}_C))\\ \text{imag}(\tilde{\boldsymbol{R}}_C/\text{norm}(\tilde{\boldsymbol{R}}_C))\end{bmatrix}\in\mathbb{C}^{2\times(N^2-1)N^2/2} \tag{7}$$

where R_{μ_1,μ_2} is the (μ_1,μ_2) th element of $\boldsymbol{R}_C$, real$(\cdot)$ and imag$(\cdot)$ are used to extract the real and imaginary parts of complex matrices, respectively. Normalized structure $\tilde{\boldsymbol{R}}_C/\text{norm}(\tilde{\boldsymbol{R}}_C)$ is more helpful to activate neurons.

The feature extraction process is summarized in Algorithm 1.

Algorithm 1 Input feature extraction

Input: $\boldsymbol{x}$

1. **for** $m\in[1,M]$ iterations **do** (2)
2. $\boldsymbol{C}_m\leftarrow\text{E}\{\boldsymbol{x}(n)\boldsymbol{x}^{\text{H}}(n+\tau_m)\}$
3. **end for**
4. $\boldsymbol{C}\leftarrow\boldsymbol{C}_m$ Stack the matrices according to (3)
5. $\boldsymbol{R}_C\leftarrow\boldsymbol{C}\boldsymbol{C}^{\text{H}}$ (5)
6. $\tilde{\boldsymbol{R}}_C\leftarrow$ upper right elements of $\boldsymbol{R}_C$ (6)
7. $\bar{\boldsymbol{R}}\leftarrow\text{real}(\tilde{\boldsymbol{R}}_C/\text{norm}(\tilde{\boldsymbol{R}}_C)),\text{imag}(\tilde{\boldsymbol{R}}_C/\text{norm}(\tilde{\boldsymbol{R}}_C))$ Real-valued transform in (7)
8. **return** $\bar{\boldsymbol{R}}$

3.2 Deep residual convolutional network based DOA estimation

We designed a DRN to learn the mapping relationship between the input feature $\bar{\boldsymbol{R}}$ and the super-resolution spectrum. By adopting the residual blocks to drive subsequent layers, a deeper network can be easily built. The information mapping path of the residual block [30] helps to optimize the network.

As shown in Fig. 1, we first use a 1D convolutional layer to extract an input feature map for the first residual block. We then insert two residual units, an identity shortcut and a projection shortcut. In the final, we adopt a full-connected layer to obtain spectral output $\hat{\boldsymbol{Q}}$. The ReLU function is employed to introduce non-linear factors to all layers.

We divide the space into a number of disjoint uniform grids according to a certain angular interval $\Delta\varsigma$. Angles in the same grid are regarded as the same category, while angles in different grids are regarded as different categories.

Fig. 2 shows the training and estimation processes of the proposed method. In the training stage, if there is an incident signal in a certain angle area, the output value of the grid corresponding to this area is 1, otherwise the output value is 0. Based on the above strategy, we can get the spectrum label $\boldsymbol{Q}_g$, so as to gain the data-label set RQ_{set} with G samples:

$$RQ_{\text{set}}=\{(\bar{\boldsymbol{R}}_1,\boldsymbol{Q}_1),(\bar{\boldsymbol{R}}_2,\boldsymbol{Q}_2),\cdots,(\bar{\boldsymbol{R}}_g,\boldsymbol{Q}_g),\cdots,(\bar{\boldsymbol{R}}_G,\boldsymbol{Q}_G)\}. \tag{8}$$

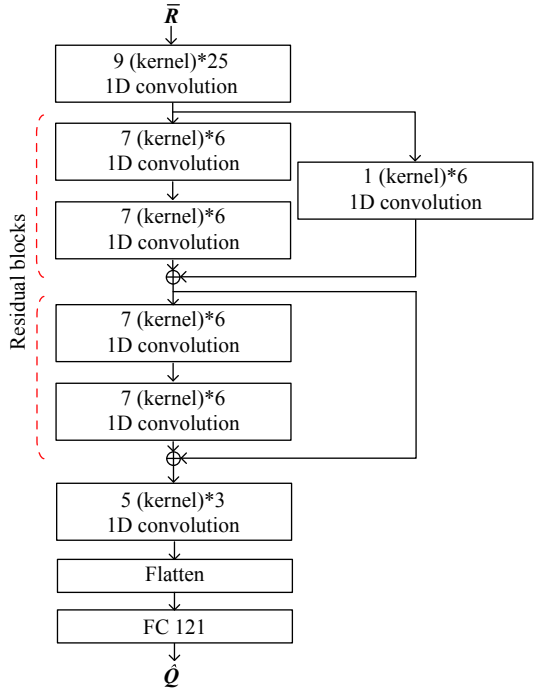

Fig. 1 Structure of the designed DRN

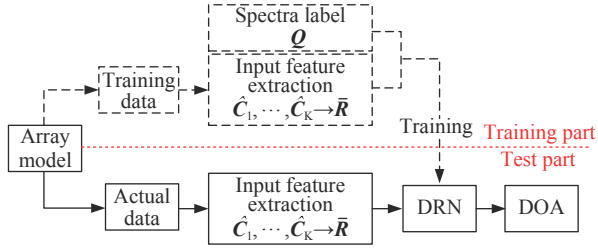

Fig. 2 Process of the proposed method

We can obtain the needed DRN by minimizing the squared l_2-norm distance between $\boldsymbol{Q}_g$ and the recovery spectra $\hat{\boldsymbol{Q}}_g$ in the training procedure, i.e.,

$$\hat{\kappa}=\arg\min_{\kappa}\frac{1}{2}\sum_{g=1}^{G}\left\|\hat{\boldsymbol{Q}}_g-\boldsymbol{Q}_g\right\|^2 \tag{9}$$

where $\hat{\kappa}$ represents the weight set. We apply the Adam algorithm with momentum and adaptive learning rate to speed up the convergence of DRN.

In the estimation stage, when a signal with unknown direction is incident on the ULA, the trained network will output the corresponding value of each grid to form a spatial spectrum. Then, we can use amplitude interpolation to improve the estimation accuracy. The angle $\hat{\theta}_j$ with higher precision is constructed by the following process:

$$\begin{cases} \dfrac{\varsigma_{e+1}-\theta_j}{\theta_j-\varsigma_e}=\dfrac{\hat{Q}_{g,e}}{\hat{Q}_{g,e+1}}, & \hat{Q}_{g,e-1}\leqslant\hat{Q}_{g,e+1} \\ \dfrac{\varsigma_e-\theta_j}{\theta_j-\varsigma_{e-1}}=\dfrac{\hat{Q}_{g,e-1}}{\hat{Q}_{g,e}}, & \hat{Q}_{g,e-1}>\hat{Q}_{g,e+1} \end{cases}, \tag{10}$$

$$\hat{\theta}_j=\begin{cases} \dfrac{\hat{Q}_{g,e}}{\hat{Q}_{g,e}+\hat{Q}_{g,e+1}}\varsigma_e+\dfrac{\hat{Q}_{g,e+1}}{\hat{Q}_{g,e}+\hat{Q}_{g,e+1}}\varsigma_{e+1}, & \hat{Q}_{g,e-1}\leqslant\hat{Q}_{g,e+1} \\ \dfrac{\hat{Q}_{g,e}}{\hat{Q}_{g,e}+\hat{Q}_{g,e-1}}\varsigma_e+\dfrac{\hat{Q}_{g,e-1}}{\hat{Q}_{g,e}+\hat{Q}_{g,e-1}}\varsigma_{e-1}, & \hat{Q}_{g,e-1}>\hat{Q}_{g,e+1} \end{cases}, \tag{11}$$

where e represents the number of grids, angle ς_e corresponds to the peak of $\hat{\boldsymbol{Q}}_g$, ς_{e-1} and ς_{e+1} are the adjacent angles of ς_e. $\hat{Q}_{g,e}$, $\hat{Q}_{g,e-1}$, and $\hat{Q}_{g,e+1}$ represent the amplitudes of ς_e, ς_{e-1}, and ς_{e+1} respectively.

The proposed algorithm is operated in the following steps.

Step 1 Calculate covariance matrices $\boldsymbol{C}_1,\boldsymbol{C}_2,\cdots,\boldsymbol{C}_M$. These matrices can only be estimated by $\hat{\boldsymbol{C}}_m=\dfrac{1}{B-\tau_k}\sum_{t=1}^{B-\tau_m}\boldsymbol{x}(t)\boldsymbol{x}^{\mathrm{H}}(t+\tau_m)$ in practice.

Step 2 Construct the matrix $\hat{\boldsymbol{C}}$ via $\left(\hat{\boldsymbol{C}}\right)_{(i-1)\times N+j,m}=\left(\hat{\boldsymbol{C}}_m\right)_{ij}$ and use the upper triangular elements of $\hat{\boldsymbol{R}}_{\boldsymbol{C}}=\hat{\boldsymbol{C}}\hat{\boldsymbol{C}}^{\mathrm{H}}$ to define the input feature $\bar{\boldsymbol{R}}$ of the DNN.

Step 3 Send features extracted from the training data to the designed DRN for training. The network learns the mapping relationship between $\bar{\boldsymbol{R}}$ and the super-resolution spectrum $\boldsymbol{Q}$. Then estimate the spectrum via the trained network. In the end, the amplitude interpolation strategy is adopted to obtain the final angle with higher precision on the estimated spectrum $\hat{\boldsymbol{Q}}$.

3.3 Computational complexity

In this subsection, we compare the computational complexity between FO-MUSIC and the proposed algorithm during the construction of the cumulant matrix and angle estimation.

The covariance matrix in the FO-MUSIC is constructed by $N^2\times N^2$ FO cumulant, thus its computational complexity can be approximately expressed as $O(9N^4B)$. The covariance matrix $\boldsymbol{R}_{\boldsymbol{C}}$ in the proposed method is constructed by M covariance matrices, thus its computational complexity can be approximately expressed as $O(MN^2B)$.

In the estimation part, the computational complexity of the MUSIC algorithm is mainly concentrated in the matrix eigenvalue decomposition and the peak search operation. Its computational complexity can be approximately expressed as

$$\mathrm{Cal}_{\mathrm{MUSIC}}=O(4MNN_\theta)+O\left(4M^2N_\theta\right)+O\left(4M^3\right) \tag{12}$$

where N_θ is the total number of the search angle related to angle range and search interval, i.e., the number of iterative operations. In general, this parameter is set to a large value for achieving precise estimation. For the DRN in Fig. 1, the overall computational complexity is determined by the size of input feature, the number and size of convolution kernels, the length of convolution steps, the number of fully connected layer nodes and the number of network layers. Thus the computational complexity of the entire DRN in Fig. 1 can be expressed as

$$\mathrm{Cal}_{\mathrm{DRN}}=\sum_{l=1}^{L_{\mathrm{DRN}}}\mathrm{Ch}_{\mathrm{in}}K_C\mathrm{Ch}_{\mathrm{out}}W_{\mathrm{out}}+H_{\mathrm{out}-1}H_{\mathrm{out}} \tag{13}$$

where L_{DRN} represents the total number of convolution layers, K_C represents the size of convolution kernel, $\mathrm{Ch}_{\mathrm{in}}$ represents the number of input channels of the lth layer, $\mathrm{Ch}_{\mathrm{out}}$ represents the number of output channels, i.e., the number of convolution kernels, W_{out} represents the size of a single channel output, $H_{\mathrm{out}-1}$ represents the number of nodes of the $(\mathrm{out}-1)$th fully connected layer, and H_{out} represents the number of output nodes. The estimation of the proposed method adopts the end-to-end DL strategy, so there is no need to perform complex calculations, such as matrix inversion, eigenvalue decomposition, or repeated iterative operations to complete the angle estimation.

Based on the analyses above, we can conclude that the proposed algorithm is computationally cheaper than the FO-MUSIC algorithm, and this advantage grows more prominent as the BSL increases. Moreover, for achieving accuracy cumulant estimations, the growth of BSL and computational load will be stronger with the increase of the order. We will quantitatively analyze the computational complexity of each method by comparing the average running time in Subsection 4.2.

3.4 Estimable signals number

The number of sources that the proposed method can estimate depends on both the feature extraction process and the limitation of the DL-based algorithm itself.

As for the SO-based methods, Congedo et al. [26] and Zhu et al. [28] have inferred that the maximum number of estimable signals can be calculated according to the expression

$$2J(J-1)\leqslant N^2(N-1)^2 \tag{14}$$

where $J\leqslant\min(N^2,M)$. If J meets the condition in (14), $\boldsymbol{C}$ will be full rank (the rank is equal to J).

DNN are very sensitive to datasets. As the number of

sources increases, the training set becomes huger and huger for complete training. The samples corresponding to multitudinous angular combinations are adverse to the "classification" learning of the DRN (In fact, the DL-based DOA estimation strategy can be regarded as a deformation of the classification idea.) and thereby could lead to difficulty in convergence. At the same time, the increase of sample volume puts higher requirements on the performance of existing equipment. Therefore, in practical application, the number of sources that can be estimated through a single network is less than the theoretical maximum in (14).

4. Simulation

We conduct a series of simulations to demonstrate the superior performance of the proposed method compared to the SO underdetermined MUSIC (SOU-MUSIC) algorithm [28], the FO-MUSIC algorithm and DRN methods based input features in [18] and [23] under overdetermined and underdetermined conditions.

4.1 Experimental setup and DRN training

We generate the training dataset by simulation. The number of sources is assumed to be known beforehand. Traditional methods such as the Akaike information criterion (AIC) [31] or the minimum description length (MDL) [32] can be used in practice to estimate the number of sources. Source-number estimation is not the focus of this work, so that process is not discussed here.

We assume that two binary phase shif keying (BPSK) modulated signals, with the radio frequencies 1 000.1 MHz and 1 000.4 MHz, impinge on the three-sensor ULA. The bit rates are all 200 kbps. To minimize the sampling rate and computational cost, the radio frequency signals are transformed into intermediate frequency signals with frequencies of 500 kHz and 750 kHz, respectively, and a sampling rate of 4 MHz. The signals simulated are all far-field, narrow-band plane waves. M is equal to 10 in the following simulation experiments.

The space of interest, $[-60°,60°]$, is divided into 121 spectrum grid units with the interval of 1°, thus the length of $\boldsymbol{Q}$ is 121. The value of the angular separation $\Delta\varphi$ is fetched from the set $\{2°,4°,\cdots,40°\}$. We take out the angle of the first signal, with the interval of 1°, within $[-60°,60°-\Delta\varphi]$, while we take out the angle of the second, with the interval of 1°, within $[-60°+\Delta\varphi,60°]$. The BSL is set to 128. The SNRs of both signals are randomly generated from $[-10\text{ dB},0\text{ dB}]$. After added with different Gaussian white noises, ten groups of different covariance vectors are collected for each set of samples. In total, we collect 20 000 samples for network training.

The training process of DRN is performed offline. A total of 20% samples of the training set are set aside randomly to construct the validation set. The initial learning rate of Adam is 0.01. The number of epoch is set to 300, and the size of mini-batch is set to 256. We shuffle the training sample set after each epoch.

We compare the proposed $\bar{\boldsymbol{R}}$ with other input features $\bar{\boldsymbol{R}}_r$ [18] and $\bar{\boldsymbol{R}}_{sp}$ [23] in terms of the boost to network training. Considering the size of the first layer of the DRN, we set $M=4,N=2$ when the input feature is $\bar{\boldsymbol{R}}_r$. The training and validation mean square errors (MSEs) varying with epochs are shown in Fig. 3.

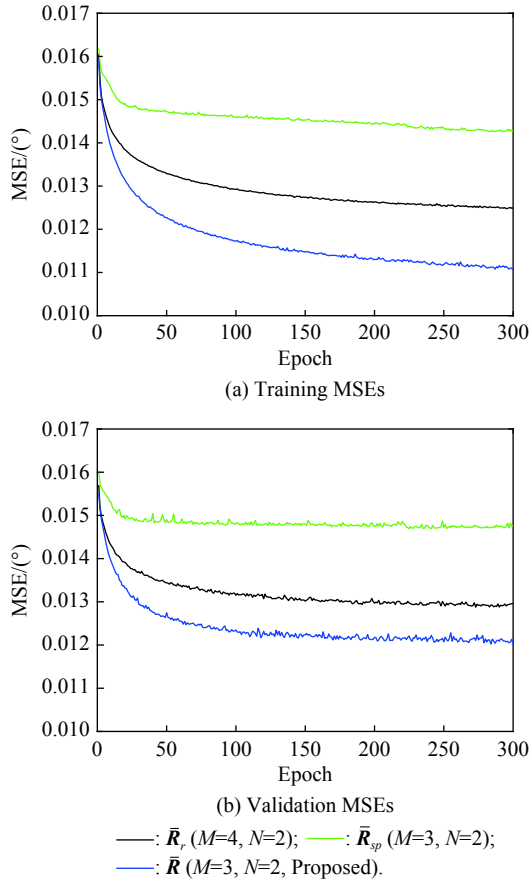

Fig. 3 Training MSEs and validation MSEs of networks with different input features (two sources)

The biggest difference between the proposed method and other DL-based DOA estimation methods is the feature extraction procedure. As shown in Fig. 3, the proposed $\bar{\boldsymbol{R}}$ brings the fastest convergence speed and the lowest MSE to the entire training process. This indicates that the input feature of the proposed method retains more angle information that is conducive to network training by comparison. There is a certain aperture expansion that occurs as well. The extraction process results in the same extended steering matrix as the method in [23], but the proposed transformation process introduces more infor-

mation useful for DRN learning.

The proposed feature extraction method can also assist the network in realizing DOA estimation under underdetermined conditions, which is not possible with data-driven methods based on ULAs. We will give verification experiments in Subsection 4.4.

4.2 Computational complexity analysis

In this subsection, we assess the computational complexity of networks with different input features and compare them with SOU-MUSIC and FO-MUSIC.

The input dimension, the trainable parameters number and the averaged training time need for these three DRN-based methods are recorded in Table 1.

Table 1 Complexity and averaged training time

Parameter	$\bar{\boldsymbol{R}}$-DRN	$\bar{\boldsymbol{R}}_r$-DRN	$\bar{\boldsymbol{R}}_{sp}$-DRN
Input dimension	2×36	1×12	2×121
Total parameters	14 291	5 354	45 146
Training time	10 min 25 s	3 min 15 s	25 min 10 s

Compared with $\bar{\boldsymbol{R}}_r$-DRN, the proposed $\bar{\boldsymbol{R}}$-DRN has longer training time because of more training parameters, whereas it has a better training effect than the other two algorithms according to Fig. 3.

The mean test time of methods for 400 trials under different BSLs is shown in Fig. 4. The computation time varies more obviously as a function of BSL than other parameters. The incident directions of the two signals with SNR=5 dB are $-9.25°$ and $7.75°$, respectively. As shown in Fig. 4, a larger BSL increases the computational load of a single test. The proposed DRN-based method does not require complex calculations or a large number of iterative operations for angle estimation, so it is quicker and less computationally burdensome than FO-MUSIC and SOU-MUSIC. The SOU-MUSIC appears to be computationally more inexpensive than FO-MUSIC, especially when the bit sequences are long, because the computing procedure based on the SO statistics requires less calculation amount than that based on the FO cumulant. In scenarios with BSL under 64, the proposed method takes time comparable to the other DRN-based methods. When the BSL becomes larger, the computational complexity of the proposed method gets slightly higher than that of the other DRN-based methods because of iteration computations of spatial covariance matrices, but the training performance of the proposed method is much better according to Fig. 3.

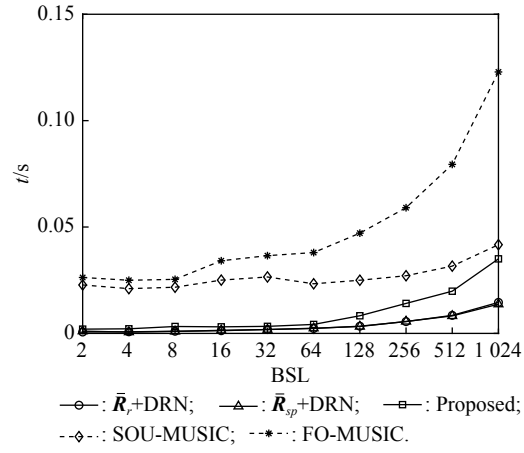

Fig. 4 Computation time vs BSL (SNR = 5 dB)

4.3 Robustness

In this subsection, we compare the robustness of the proposed method with that of SOU-MUSIC and FO-MUSIC under different angle separation, BSL, and SNR conditions.

We use the average root mean square error (RMSE) of the DOA estimation as a performance indicator: RMSE = $\sqrt{\frac{1}{HJ}\sum_{h=1}^{H}\left\|\hat{\boldsymbol{\theta}}^h-\boldsymbol{\theta}^h\right\|^2}$, where H represents the Monte-Carlo trial number, $\hat{\boldsymbol{\theta}}^h$ and $\boldsymbol{\theta}^h$ represent the estimation angle and the true angle in the hth Monte-Carlo trial respectively, and J represents the number of signals. We conduct Monte-Carlo experiments consisting of 400 runs in the subsequent simulations. To intuitively display the RMSE curves, we set the search interval of all model-driven methods to $0.1°$.

Fig. 5 shows the RMSE as a function of the angle separation when the BSL is 128 and SNR is 5 dB. Two signals impinge onto the ULA from $-5.25°+\phi$ and $-5.25°+\phi+\Delta\varphi$, with $\phi(-0.5°,0.5°)$, respectively. The set of angular distances in this case is $[2°,3°,\cdots,10°]$.

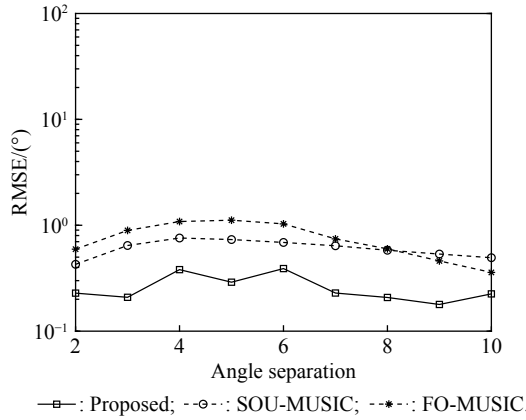

Fig. 5 RMSE vs angle separation (BSL=128, SNR=5 dB)

As can be seen in Fig. 5, the RMSEs of the proposed method are all within 0.4° while the RMSEs of the other two methods are larger, indicating that the super-resolution capability of the proposed method is the best among them.

Fig. 6 shows the RMSE as a function of BSL when the SNR is 5dB. The directions of two signals are set to −9.25° and 7.75°, respectively. As shown in Fig. 6, the proposed algorithm is more accurate than FO-MUSIC and SOU-MUSIC when the BSL is small.

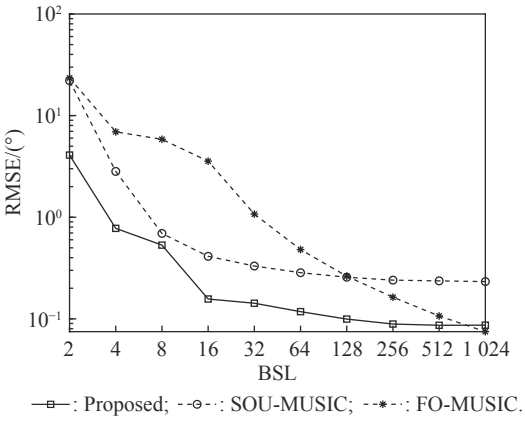

Fig. 6 RMSE vs BSL (SNR = 5 dB)

Synthesizing the results in Fig. 4 and Fig. 6, when the BSL is less than about 128, the proposed method has advantages in estimation accuracy and time consumption, compared with the other two methods. As the BSL increases, the proposed method offers a slightly lower precision than the FO-MUSIC method, but still consumes much fewer computational resources. Its efficiency makes the proposed method especially well-suited to real-time DOA estimation applications.

Fig. 7 shows the RMSE as a function of the SNR when the BSL is 256 and signal directions are fixed to −5.75° and 11.25°. Increasing the SNR usually enhances DOA estimation performance, which is also the case here. The estimation precision of the proposed method over the other two methods is significant when the SNR is low. When the SNRs of the incident signals are higher than 8 dB, the proposed method performs slightly worse than other two methods, but with much lower computation consumption. In scenarios with high SNRs, the coarser spatial grids (i.e. an interval of 1°) limit the estimation accuracy of the proposed method. Further, the SNR of the test set cannot be kept consistent with that of the training set once it reaches a certain level, so there is a certain deviation between the test set and the training set. These constraints drive down the estimation performance of the proposed method to the point where the curve changes with SNR are no longer obvious.

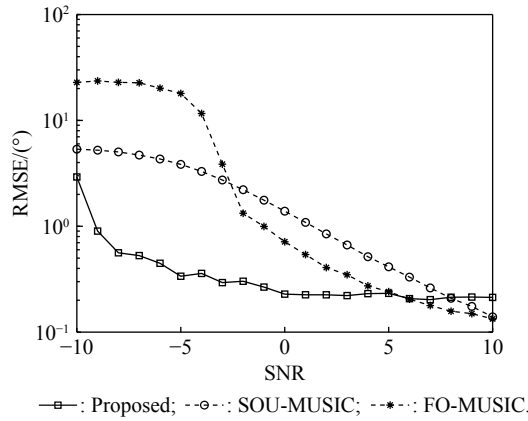

Fig. 7 RMSE vs SNR (BSL= 256)

4.4 DOA estimation performance under underdetermined conditions

In this subsection, we compare the DOA estimation performance of the proposed method with that of SOU-MUSIC [28] and FO-MUSIC under underdetermined conditions.

We first observe the contribution of the SO statistic of the proposed method with that of the FO statistic on DOA estimation. Zhu et al. [28] has infirmed that this kind of the SO statistic-based algorithm requires fewer bits than the FO statistic-based algorithm for accurate angle estimation under underdetermined conditions. We further reduce the BSL 1−2 orders of magnitudes and use the traditional MUSIC method to obtain the pseudo-spectrum. As shown in Fig. 8, the peaks of the SO-based pseudo-spectrum we gather become more sleek, but directions can still be roughly distinguished. This is enough to indicate that the SO-statistic of the proposed method can parse out more useful information, which is more helpful to DRN training.

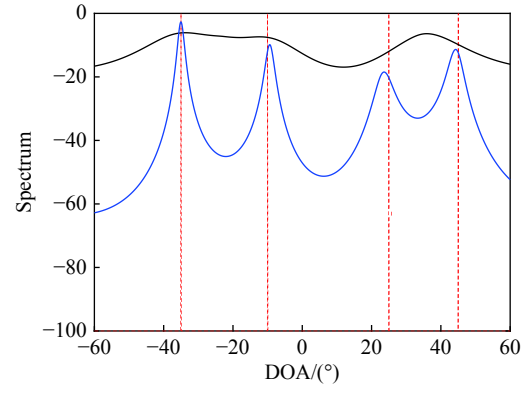

(a) BSL=32

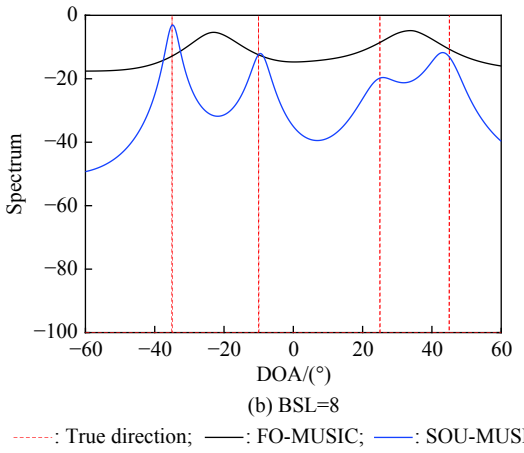

Fig. 8 Pseudo-spectrum for SOU-MUSIC and FO-MUSIC (four sources, three sensors)

We next test the proposed DOA estimation method under underdetermined conditions. We retrain the networks in the case of four sources and set the angular distances between two adjacent signals to $\{2^\circ, 4^\circ, \cdots, 10^\circ\}$. SNR is set consistently to 5 dB. The covariance matrices are obtained from bit sequences with a length of 128. Fifteen groups of different covariance vectors are collected for each set of samples.

The training and validation MSEs varying with epochs are shown in Fig. 9.

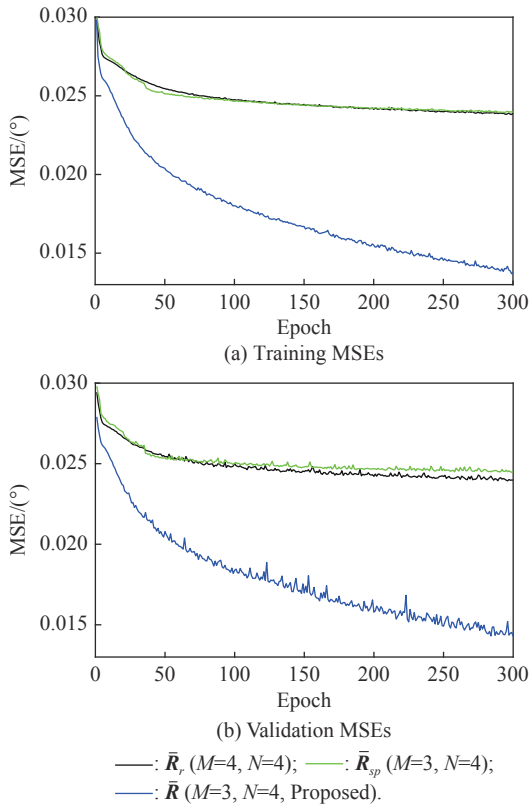

Fig. 9 Training and validation MSEs of networks with different input features (four sources)

The DRN with $\bar{\boldsymbol{R}}$ constructed via the SO statistic shows the strongest performance. Under underdetermined conditions, $\bar{\boldsymbol{R}}$ makes the difference between samples more obvious, thereby reducing the difficulty of DRN training, which is conducive to the network's learning of the non-linear mapping relation between $\bar{\boldsymbol{R}}$ and $\boldsymbol{Q}$.

As shown in Fig. 10, four signals are assumed to impinge onto the array from -11.5°, -2.5°, 4.5°, and 9.5°, respectively. We normalize the spatial spectrums of SOU-MUSIC and FO-MUSIC. In the case of closer angular intervals, the proposed method successfully estimates all angles while two model-based methods fail to do so. Thus, the proposed method achieves a higher angular resolution in underdetermined cases. As for the other two DRN-based methods, their estimation results are unsatisfactory. Interestingly, their spectral peaks are concentrated near the true value. This is due to the data-based characteristics of the neural network. The two DRN-based methods learn mapping relationships based on the training sets, but those relationships are not sufficiently accurate enough due to a lack of information provided by $\bar{\boldsymbol{R}}_r$ and $\bar{\boldsymbol{R}}_{sp}$ under underdetermined conditions.

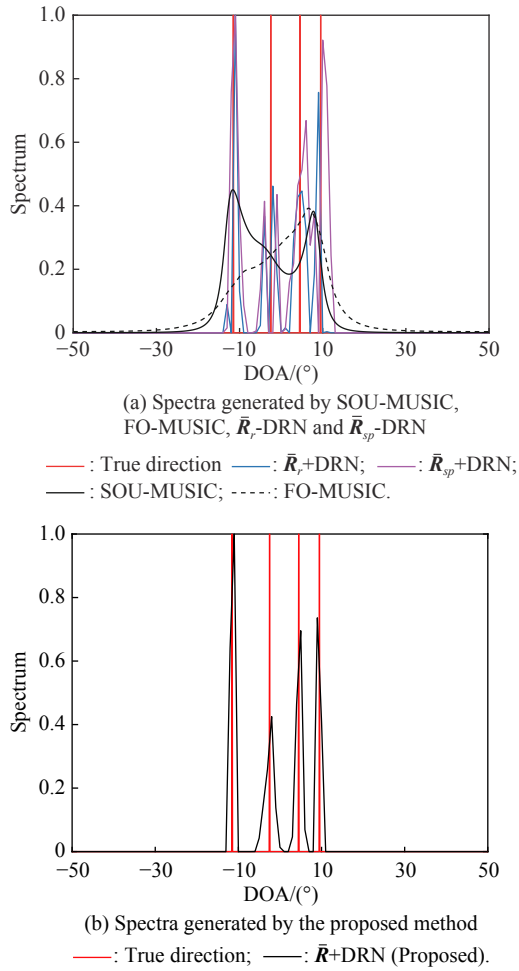

Fig. 10 Spectra comparison under underdetermined conditions (four sources)

In summary, results show that the SO statistic in the proposed method reveals more angle information within limited BSL. Thus, the input features extracted based on the proposed method are more conducive to the network training of underdetermined DOA estimation than the other methods we test in this study.

5. Conclusions

This paper proposes a DL-based DOA estimation method for underdetermined cases that is designed to exploit differences in covariance matrices. The proposed algorithm uses an input feature extraction method based on multiple time-delay covariance matrices. A deep convolutional network with residual blocks then learns the non-linear mapping from the input feature to the spatial spectrum. Finally, amplitude interpolation is used to refine the DOA estimation. Simulations show that the proposed algorithm has competitive or even better DOA estimation performance and computational efficacy under both overdetermined and underdetermined conditions compared to other state-of-the-art methods.

Nevertheless, only if the practice number of signals is equivalent to the number in training, will the proposed approach show the best estimation results. We also find that simply expanding the size of sample sets to estimate more sources may result in a heavy computational burden and impede the effective convergence of the single network. In practice, it would be necessary to split incident signals after estimating the number of sources to adapt to the trained network with a fixed source number. Therefore, apart from enhancing the calculated performance of equipment, we plan to explore a signal division tactics for parallel network training in the future.

References

[1] VEEN B V, BUCKLEY K M. Beamforming: a versatile approach to spatial filtering. IEEE ASSP Magazine, 2002, 5(2): 4–24.

[2] LIU Z M, HUANG Z T, ZHOU Y Y. An efficient maximum likelihood method for direction-of-arrival estimation via sparse Bayesian learning. IEEE Trans. on Wireless Communications, 2012, 11(10): 1–11.

[3] SCHMIDT R, SCHMIDT R O. Multiple emitter location and signal parameter estimation. IEEE Trans. on Antennas and Propagation, 1986, 34(3): 276–280.

[4] ROY R, PAULRAJ A, KAILATH T. ESPRIT—a subspace rotation approach to estimation of parameters of cisoids in noise. IEEE Trans. on Acoustics, Speech and Signal Processing, 1986, 34(5): 1340–1342.

[5] YIN J H, CHEN T Q. Direction-of-arrival estimation using a sparse representation of array covariance vectors. IEEE Trans. on Signal Processing, 2011, 59(9): 4489–4493.

[6] LIU Z M, HUANG Z T, ZHOU Y Y. Sparsity-inducing direction finding for narrowband and wideband signals based on array covariance vectors. IEEE Trans. on Wireless Communications, 2013, 12(8): 3896–3907.

[7] PORAT B, FRIEDLANDER B. Direction finding algorithms based on high-order statistics. IEEE Trans. on Signal Processing, 1991, 39(9): 2016–2024.

[8] CHEVALIER P, FERREOL A, ALBERA L. High-resolution direction finding from higher order statistics: the 2q-MUSIC algorithm. IEEE Trans. on Signal Processing, 2006, 54(8): 2986–2997.

[9] LIU T H, MENDEL J M. A subspace-based direction finding algorithm using fractional lower order statistics. IEEE Trans. on Signal Processing, 2001, 49(8): 1605–1613.

[10] RICKARD S, DIETRICH F. DOA estimation of many W-disjoint orthogonal sources from two mixtures using DUET. Proc. of the IEEE 10th Workshop on Statistical Signal and Array Processing, 2000: 311−314.

[11] TADAION A A, DERAKHTIAN M, GAZOR S. A fast multiple-source detection and localization array signal processing algorithm using the spatial filtering and ML approach. IEEE Trans. on Signal Processing, 2007, 55(5): 1815–1827.

[12] ZHENG Z, LI G J, TENG Y L. 2D DOA estimator for multiple coherently distributed sources using modified propagator. Circuits Systems & Signal Processing, 2012, 31(1): 255–270.

[13] HAN P, WANG D M, CUI W J, et al. Underdetermined direction of arrival estimation of non-circular signals via matrix completion in nested array. IEEE Access, 2019, 7: 183717–183728.

[14] YADAV S K, GEORGE N V. Underdetermined direction-of-arrival estimation using sparse circular arrays on a rotating platform. IEEE Signal Processing Letters, 2021, 28: 862–866.

[15] HE W, MOTLICEK P, ODOBEZ J M. Deep neural networks for multiple speaker detection and localization. Proc. of the IEEE International Conference on Robotics and Automation, 2018: 74−79.

[16] HUANG H J, YANG J, HUANG H, et al. Deep learning for super-resolution channel estimation and DOA estimation based massive MIMO system. IEEE Trans. on Vehicular Technology, 2018, 67(9): 8549–8560.

[17] MA N, MAY T, BROWN G J. Exploiting deep neural networks and head movements for robust binaural localization of multiple sources in Reverberant environments. IEEE Trans. on Audio Speech and Language Processing, 2017, 7(19): 123–132.

[18] LIU Z M, ZHANG C W, YU P S. Direction-of-arrival estimation based on deep neural networks with robustness to array imperfections. IEEE Trans. on Antennas and Propagation, 2018, 66(12): 7315–7327.

[19] ABEYWICKRAMA S, JAYASINGHE L, FU H. RF-based direction finding of UAVs using DNN. Proc. of the IEEE International Conference on Communication Systems, 2018: 903−912.

[20] XIANG H H, CHEN B X, YANG M L. Altitude measurement based on characteristics reversal by deep neural network for VHF radar. IET Radar, Sonar & Navigation, 2019, 13(1): 98–103.

[21] XIANG H H, CHEN B X, YANG T. Improved de-multipath neural network models with self-paced feature-to-feature learning for DOA estimation in multipath environment. IEEE Trans. on Vehicular Technology, 2020, 69(5): 5068–5078.

[22] XIANG H H, CHEN B X, YANG M L, et al. A novel phase enhancement method for low-angle estimation based on supervised DNN learning. IEEE Access, 2019, 7(4): 329–336.

[23] WU L L, LIU Z M, HUANG Z T. Deep convolution network for direction of arrival estimation with sparse prior.

IEEE Signal Processing Letters, 2019, 26(11): 1688–1692.
[24] GUO Y, ZHANG Z, HUANG Y Z. DOA estimation method based on cascaded neural network for two closely spaced sources. IEEE Signal Processing Letters, 2020, 27(1): 570–574.
[25] CHEN Y, WANG C, XIONG K L. Synchronized perturbation elimination and DOA estimation via signal selection mechanism and parallel deep capsule networks in multipath environment. Chinese Journal of Aeronautics, 2021. DOI: 10.1016/J.CJA.2021.01.016.
[26] CONGEDO M, GOUY-PAILLER C, JUTTEN C. On the blind source separation of human electroencephalogram by approximate joint diagonalization of second order statistics. Clinical Neurophysiology, 2008, 119 (12): 2677–2686.
[27] LATHAUWER L D, CASTAING J. Blind identification of underdetermined mixtures by simultaneous matrix diagonalization. IEEE Trans. on Signal Processing, 2008, 56(3): 1096–1105.
[28] ZHU L W, WANG Y, WANG X, et al. Underdetermined direction-of-arrival estimation from second order statistics. Proc. of the 7th International Congress on Image and Signal Processing, 2014: 989−993.
[29] CHEN Y, XIONG K L, HUANG Z T. Robust direction-of-arrival estimation via sparse representation and deep residual convolutional network for co-prime arrays. Proc. of the IEEE 3rd International Conference on Electronic Information and Communication Technology, 2020: 514−519.
[30] HE K M, ZHANG X Y, REN S Q, et al. Deep residual learning for image recognition. Proc. of the IEEE Conference on Computer Vision and Pattern Recognition, 2016: 770−778.
[31] SEGHOUANE A K. Asymptotic bootstrap corrections of AIC for linear regression models. Signal Processing, 2010, 90(1): 217–224.
[32] STOICA P, SELEN Y. Model-order selection: a review of information criterion rules. IEEE Signal Processing Magazine, 2004, 21(4): 36–47.

Biographies

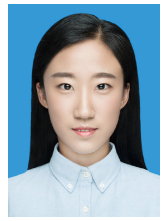

CHEN Ying was born in 1995. She is a Ph.D. student in the State Key Laboratory of Complex Electromagnetic Environment Effects on Electronics and Information System, National University of Defense Technology. Her research interests are array signal processing and deep learning.
E-mail: chenying_nudt@163.com

WANG Xiang was born in 1985. He received his B.S. and Ph.D. degrees in information and communication engineering in 2007 and 2013, respectively, from the College of Electronic Science and Engineering, National University of Defense Technology, Changsha, Hunan, China. Currently, he is a lecturer in the National University of Defense Technology, Changsha, Hunan, China His research interests include blind signal separation and non-cooperative signal processing in radar and communication applications.
E-mail: christopherwx@163.com

HUANG Zhitao was born in 1976. He received his B.S. and Ph.D. degrees in information and communication engineering in 1998 and 2003, respectively, from the College of Electronic Science and Engineering, National University of Defense Technology, Changsha, Hunan, China. He is now a professor with the College of Electronic Science and Engineering, National University of Defense Technology, Changsha, Hunan, China. His research interests include radar and communication signal processing, and array signal processing.
E-mail: tald_paper@163.com